# Effect of Particle Addition to Liquid Metal on Fabrication of Aluminum Foam

Kota Kadoi[1] and Hideo Nakae[2]

[1] *Graduate Student, Dept. of Materials Science and Engineering, Waseda Univ.*
[2] *Dept. of Materials Science and Engineering, Waseda Univ.*

(Received March 30, 2006; final form April 10, 2006)

## ABSTRACT

Aluminum foams are very attractive materials for automobile and aerospace applications, where the weight reduction and the improvement in safety devices as energy absorbing materials are requested. These advantages should be affected by the size of the foam cell, namely, the smaller the better. Therefore, we shall discuss how to make finer foams. The most popular fabrication process of aluminum foams is particle decomposition in the melt process using $TiH_2$ powder addition. In this study, by using an aqueous solution as a visible model, dynamic changes in the shape of the meniscus and the force which acts on a particle were examined as a function of the contact angle during the transfer process. We propose a model which can estimate the force necessary to entrap the particle in the liquid. Furthermore, the optimum stirring conditions for entrapping the particle and for uniformly dispersing it in the liquid were also investigated using the visible model. During the fabrication of the aluminum foams, as the starting materials, pure aluminum and Al-12.6Si alloys were used. The viscosity of these alloys increased to the objective value by the addition of Ca and aluminum powder, then $TiH_2$ powder was added to the melts using the pre-optimized stirring conditions. It was found that the number of cells per unit area and the cell wall thickness were determined by the viscosity of the molten alloys.

**Keywords;** aluminum foams, viscosity, powder addition, particle addition.

## 1. INTRODUCTION

The significant features of closed cell aluminum foams are their low density, high specific strength, high energy absorption, etc. /1,2,3/ Most of the closed cell aluminum foams are produced by adding foaming agents to the aluminum melt while stirring /1,4/ followed by particle decomposition in the melt process. Due to these advantages, aluminum foams are very attractive materials for automobile and aerospace applications, where the weight reduction and the improvement in safety devices are requested. These properties of the foam such as energy absorption, etc., are affected by the size of the foam bubbles, namely, the smaller the better /5,6/.

In order to obtain finer bubble foams, as the first step, an effective particle addition process, such as $TiH_2$ powder into the molten aluminum alloys, is necessary. In this study, from a fundamental viewpoint, the dynamic change in the force which works on the particle during immersion was examined. Observations of the meniscus shape around the particle were carried out /7,8/. Based on these observations, changes in the shape of the meniscus are summarized as a "particle transfer model with contact angle". The total force, which works on the particle due to the surface tension, $F_t$, and gravity, $F_g$, was then estimated as a function of the contact angle. In order to confirm the validity of this estimation, the measurement of the force was also carried out by the immersion of a steel ball in an aqueous solution with various surfactants.

Besides these fundamental approaches, the optimum

stirring condition was investigated as a function of the propeller dimensions. As a secondary step, to fabricate a finer cell, it should be necessary to investigate the influence of viscosity on the stability of the film and cell size. The stability of the membrane was reported by S.W.Ip *et al* /9/. As the advantage of their aqueous solution experiment, the stability could be independently evaluated free from the solidification. In our study, the influence of the viscosity on the cell size of the aluminum foam was examined by function of the viscosity with the addition of Ca and aluminum powder with stirring.

## 2. OBSERVATION OF MENISCUS AT PARTICLE/WATER INTERFACE

A ball bearing with a 1.0 mm radius, coated with paraffin, was used for the observation of the meniscus shape. The aqueous solutions were pure water and a surfactant, sodium lauryl sulfate (abbreviated SLS) added solutions, in which the surfactant contents were changed for controlling the contact angle between the paraffin and the solutions. The surface tensions of these solutions were measured by the maximum bubble pressure method, and the contact angles were measured by the sessile drop method. As the model whose contact angle is 0°, a 1 mm radius ball bearing without the coating and 0.10 mass% SLS aqueous solution was used /9/.

The measured values of the contact angle and the surface tension for each solution are shown in Table 1. The contact angles are changed by the SLS addition from the perfect wetting (0°) to non-wetting (105°) range as shown. Photos of the meniscus for two solutions are shown in Fig. 1 for the good wetting (69°) system and the poor wetting (105°) system. The ball was supported by a fine thread in order to maintain its position. As can be clearly seen, the meniscus of the good wetting system, with the contact angle of 69°, goes up, and that for the poor wetting system, with the contact angle of 105°, in which the meniscus is suppressed due to having the lowest total interfacial energy. Based on these observations, the shape of the meniscus around the particle is illustrated as shown in Fig. 2 as a function of the contact angle.

**Table 1**
Contact angles for paraffin and SLS aqueous solutions and surface tension.

| SLS, mass% | Contact angle, deg | $\gamma_{LV}$, mN/m |
|---|---|---|
| 0.00 | 105 | 69.2 |
| 0.03 | 95 | 66.9 |
| 0.10 | 90 | 62.0 |
| 0.41 | 69 | 46.5 |
| 1.03 | 58 | 34.8 |

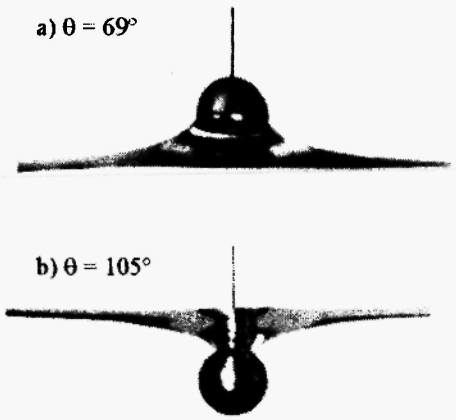


**Fig. 1:** Photos of aqueous solution meniscus on particles

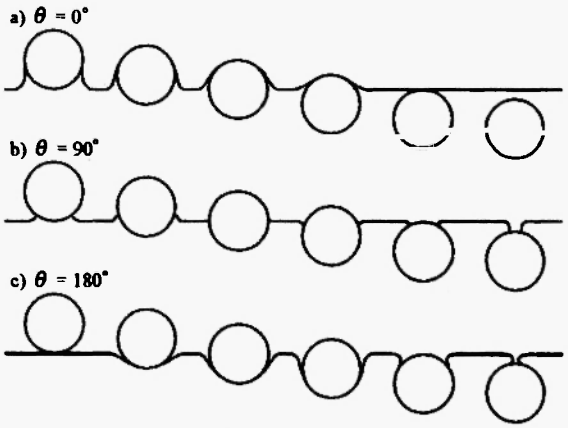


**Fig. 2:** Differences of meniscus form with wettability.

## 3. PARTICLE TRANSFER MODEL FORM VAPOR TO LIQUID

We propose a particle transfer model for the calculation of the external force, which requires the immersion of the particle into the liquid, based on the meniscus observation /9/ as shown in Fig. 3. In this model, it is assumed that the constant contact angle is independent of the depth of the dipping during the insertion process of the particle. Some other models similar to Fig. 3 were proposed by Rohatgi *et al.* /10/ using a flat liquid surface, and by Kaptay /11,12/ using an interfacial energy model. In this study, the model has been proposed and verified in order to discuss the effect of the meniscus shape and the contact angle on the particle addition.

The shape of the meniscus was taken into account in order to estimate the force acting during the particle addition, as shown in Fig.3. At the liquid / particle / vapor interface, the surface tension, $\gamma_{l,v}$, times the circumference is equal to the total force, $F_{interface}$, by the following equation /8,9/.

$$F_{interface} = 2\pi R\,\gamma_{l,v}\sin\phi\,\sin(\phi+\theta) \qquad (1)$$
$$\phi = \arccos\{(R - X')/R\}$$

where θ is the contact angle between the particle and the solution. The effect of gravity, g, namely the effect of buoyancy, $F_g$, is added to the equation, then the total force on the particle, $F_{total}$, can be calculated.

$$F_g = \pi g X^2 (3R - X)(\rho_S - \rho_L)/3 + \pi g (2R - X)^2 (R + X)(\rho_S - \rho_V)/3 \qquad (2)$$

where $\rho_S$, $\rho_l$, and $\rho_V$ are the densities of the particle, solution and vapor, respectively.

$$F_{total} = F_{interface} + F_g \qquad (3)$$

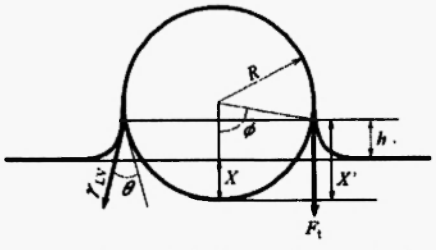


**Fig. 3:** Interfacial model of particle transfer into melt.

Fig. 4 shows the calculation result of equation (3) based on the influence of the particle size on $F_{total}$, $F_{interface}$ and $F_g$ for the $Al_2O_3$/Al system at $X/R$ = 1.5. We assumed that the surface tensions and the specific densities of the particle, melt and vapor at 1273K are as follows: $\gamma_{SL}$ = 1560 mN/m, $\gamma_{SV}$ = 1560 mN/m, $\gamma_{l,V}$ = 795 mN/m, $\rho_S$ = 3.9 g/cm$^3$, $\rho_L$ = 2.7 g/cm$^3$ and $\rho_V$ = 0 g/cm$^3$. These conditions mean that the contact angle is 90° because $\gamma_{SL}$ equals $\gamma_{SV}$. At the depth $X/R$ = 1.5, it is found that the total force depends on the size of the particle and shows a maximum excluding force near a 5 mm radius. This figure shows that if the radius is less than 1.0 mm, the total force, $F_{total}$, is mainly controlled by the interfacial energy rather than the gravitational force. This region should be called the "interfacial energy controlled region".

If the size of a particle becomes smaller, the smaller $F_{total}$ is reasonable. In order to discuss the required force per unit mass of the particle, the value, which has the unit dimension of m/s$^2$, should be a criterion of the easiness of immersion. This value is shown in Fig.4. In the case of a particle with a radius of 1 μm, the value has the order of $10^8$ m/s$^2$ which is $10^5$ times the gravitational force. Therefore, the small particle transfer is very difficult compared to that of the larger one.

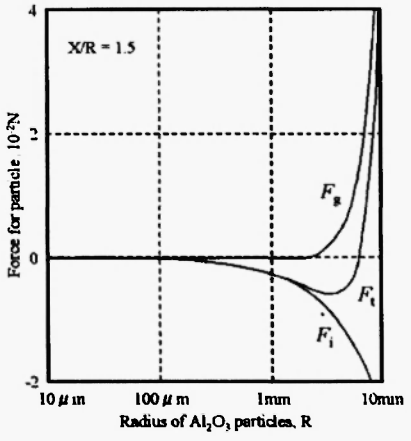


**Fig. 4:** Change in force for particle with particle radius.

For the confirmation of this model, we measured the force acting on a particle using a precise microbalance for every 0.2mm of pitch of a 1.0mm radius ball coated by paraffin The positive value indicates that the particle is forced to be included in the melt. As shown in Fig. 5, the maximum exclusion force (the minimum value) is

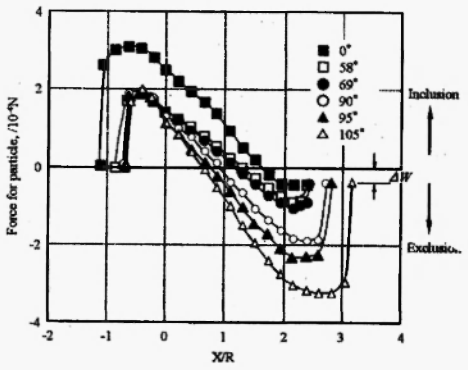


**Fig. 5:** Measured values of force acting on particles.

obtained at 2.0 – 2.5 of *X/R*. A comparison of the estimated value with the measured value, when the contact angle is 90°, is shown in Fig. 6. The experimental results show a good agreement with the calculated line using the values shown in Table 1.

## 4. OPTIMIZING THE STIRRING CONDITIONS

The surface of an aluminum melt is usually covered with a thin oxide film of $Al_2O_3$. Therefore, most of the additives, such as $TiH_2$ and aluminum powder, would be identified as non-wetting particles due to the prevention of direct contact of the aluminum melt by the film. Moreover, it is necessary to uniformly disperse the particles for the fabrication of fine aluminum foams. Thus, we investigated the optimum stirring conditions for entrapping and for uniformly dispersing the particles using the aqueous solutions model. We used Teflon particles with the diameters of 0.3, 0.5 and 1.0 mm as the non-wetting particles. The kinematic viscosity, Reynolds number and the relative density, $d_S/d_L$, are listed for the molten aluminum and pure water in Table 2. Here the outer diameter for four blades of the propeller was 61 mm and the stirring device shown in Fig. 7. Based on these values, the aqueous solution model could be used to estimate the behavior of the particles on the molten aluminum alloys.

The stirring system consists of a motor, double four-bladed propellers, a high speed video camera and a glass crucible in a square glass container filled with water for good observation without distortion of the picture. The size and shape of the glass crucible is the same as the size of the clay-bonded graphite crucible, which is used as the aluminum foam fabricating device, with the capacity of 400 ml. The movement of a Teflon particle with a 1.0 mm diameter was traced with the parameters of the blade angle of the upper propeller, $\theta_u$, and that of

**Table 2**
Physical properties of aluminum melt, water and adding particles.

| | kinematic viscosity ($m^2/s$) | Reynolds number |
|---|---|---|
| Al (933K) | $0.48 \times 10^{-6}$ | $3.5 \times 10^4$ |
| water (293K) | $1.0 \times 10^{-6}$ | $1.7 \times 10^4$ |

| | particles | $d_S/d_L$ |
|---|---|---|
| aluminum melt | $TiH_2$ | 1.9 |
| | CaO | 1.4 |
| water | Teflon | 2.0 |

$d_S$: density of particle
$d_L$: density of liquid

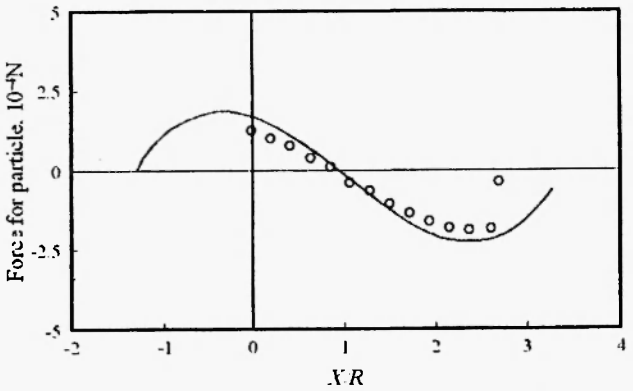


**Fig. 6:** Comparison of measured value and calculated one.

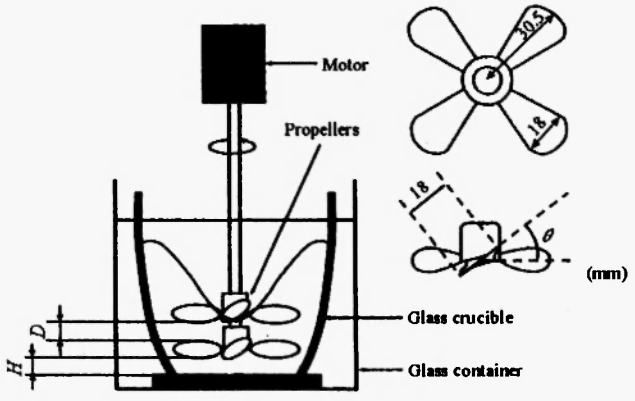


**Fig. 7:** Schematic drawing of experimental apparatus.

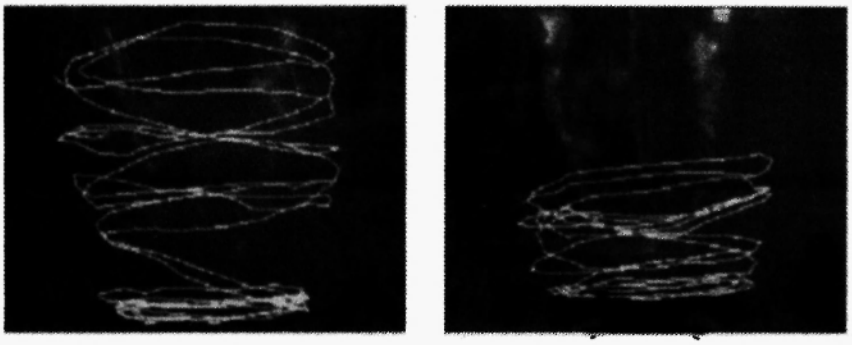

$\theta_u$ : 60°, H : 10mm, $\theta_l$ : 30°, D : 30mm

$\theta_u$ : 120°, H : 15mm, $\theta_l$ : 30°, D : 30mm

**Fig. 8:** Loci for movement of particle.

the lower one, $\theta_l$, the distance of the propellers, $D$, and the height of the lower propeller from the bottom, $H$. The dimensions of the propellers are also shown in Fig.7.

Particles cannot be entrapped in pure water without a surfactant using a single impeller. Therefore, we selected the double propeller system using a black light and fluorescence painted particle system to avoid any miss observations due to air bubbles. The movements of a particle traced by the video recorder are shown in Fig. 8 as lines. The movement of the particles was classified into four types. If the movement, namely the trace line of the particle, is very uniform, the stirring condition is identified as "very good", expressed by " ". If the particle movement located in under the upper propeller, the condition is "good" expressed by "o". Finally, if the region is limited between the upper propeller and the lower one, the condition is "not good" expressed by " ". If the movement is limited only under the lower propeller, the condition is "bad" expressed by "×". Based on these results, the optimum condition is as follows: $\theta_u$ is 60°, $\theta_l$ is 30°, $D$ is 30mm and $H$ is 10mm.

In order to examine the efficiency of the particle entrapment in the liquid, ten particles were dropped on the liquid surface and then mixed under several conditions, as shown in Table 3. After ten seconds, the particle number in the water was counted. The average number of ten trials for each condition is also listed in Table 4. From these results, it is confirmed that the efficiency of the particle entrapping are not significantly dependent on these conditions, if we used the double propeller system.

## 5. FABRICATION OF ALUMINUM FOAMS

We used a clay-bonded graphite crucible in which 400 ml of pure aluminum or Al-12.6mass%Si alloys were melted and kept at 973K and 873K, respectively. As the additives, Ca and aluminum powder for controlling the viscosity of the molten alloy and $TiH_2$ powder for the foaming agent, were used. /13,14/. We considered that the aluminum powder was covered by a thin $Al_2O_3$ film, then the film acted as a source of $Al_2O_3$ particles after being crushed. The experimental conditions are shown in Table 5. As for the viscosity, the torque of the motor was measured by a torque meter located on the shaft. The dimensions of the stirring system are identical to that of the water model system except for the ceramic coatings on the surface of the propeller with a thickness of about 0.2 mm.

The aluminum powder and Ca were added to the molten alloys to increase the viscosity. When the torque became the targeting value, $T_o$, by agitating after the addition of the Ca and aluminum powder, then the $TiH_2$ powder was added to the melt. Just after the $TiH_2$ powder addition, the crucible was removed from the furnace and cooled on the Cu plate. The influence of the viscosity on the foamability was examined based on the normalized torque, $T_o/T_b$, in which $T_b$ is the original torque of the melt before the Ca and aluminum powder addition. The changes in the torque during the stirring were monitored as shown in Fig. 9 for the pure aluminum and Al-12.6%Si alloy systems. The $T_o/T_b$ value increases about three times after 1200s of stirring. It was found that the addition of the Ca and aluminum

**Table 3**

Conditions for dispersion of Teflon particle.

| upper | lower | height | distance | dispersion |
|---|---|---|---|---|
| 30° | 30° | 5 | 40 | △ |
| | | | 30 | △ |
| | | | 20 | △ |
| 60° | 60° | 5 | 40 | △ |
| | | | 30 | △ |
| | | | 20 | △ |
| 120° | 120° | 5 | 40 | × |
| | | | 30 | × |
| | | | 20 | △ |
| 30° | 60° | 5 | 40 | × |
| | | | 30 | × |
| | | | 20 | × |
| 30° | 120° | 5 | 40 | × |
| | | | 30 | × |
| | | | 20 | × |
| 60° | 30° | 5 | 40 | ○ |
| | | | 30 | ○ |
| | | | 20 | ○ |
| 60° | 120° | 5 | 40 | × |
| | | | 30 | × |
| | | | 20 | × |
| 120° | 30° | 5 | 40 | ○ |
| | | | 30 | △ |
| | | | 20 | △ |
| 120° | 60° | 5 | 40 | ○ |
| | | | 30 | ○ |
| | | | 20 | △ |

| upper | lower | height | distance | dispersion |
|---|---|---|---|---|
| 60° | 30° | 5 | 40 | ○ |
| | | 10 | | ○ |
| | | 15 | | ○ |
| | | 5 | 30 | ○ |
| | | 10 | | ◎ |
| | | 15 | | ○ |
| | | 5 | 20 | ○ |
| | | 10 | | ○ |
| | | 15 | | △ |
| 120° | 60° | 5 | 40 | ○ |
| | | 10 | | ○ |
| | | 15 | | △ |
| | | 5 | 30 | △ |
| | | 10 | | △ |
| | | 15 | | △ |
| | | 5 | 20 | △ |
| | | 10 | | × |
| | | 15 | | × |
| 120° | 30° | 5 | 40 | ○ |
| | | 10 | | ○ |
| | | 15 | | ○ |
| | | 5 | 30 | ○ |
| | | 10 | | △ |
| | | 15 | | △ |
| | | 5 | 20 | △ |
| | | 10 | | ○ |
| | | 15 | | △ |

**Table 4**

Numbers of entrapped particles.

| | distance (mm) | | particle size | | |
|---|---|---|---|---|---|
| | | | 1.0mm | 0.5mm | 0.3mm |
| upper:60° | 20 | ○ | 10.0 | 8.4 | 7.6 |
| lower:30° | 30 | ◎ | 10.0 | 8.8 | 8.0 |
| height:10mm | 40 | ○ | 10.0 | 9.0 | 8.2 |
| upper:120° | 20 | ○ | 10.0 | 8.6 | 7.4 |
| lower:30° | 30 | △ | 10.0 | 8.8 | 7.4 |
| height:10mm | 40 | ○ | 9.8 | 8.8 | 8.0 |

**Table.5**
Experimental conditions of fabrication for aluminum foams.

| Matrix (400g) | Pure aluminum | Al-12.6%Si |
|---|---|---|
| Temperature | 973 K | 873 K |
| Aluminum powder | 10 mass% | 5 mass% |
| Ca | 0.2 mass% | 1 mass% |
| $TiH_2$ | 0.5 mass% | 0.5 mass% |

powder is an effective way to control the viscosity. Fig. 10 shows the cross sections of the foams for the pure aluminum and Al-12.6%Si alloy as the function of $T_o/T_b$. The cell size decreases with an increase in the normalized torque, namely, the viscosity. The number of cells per unit area and the cell wall thickness for the pure aluminum and Al-12.6mass%Si alloy are shown in Fig. 11 and Fig. 12, respectively. It was found that regardless of the alloys, the number of cells linearly increased and the cell wall thickness linearly decreased with an increase in the torque. Thus, a higher viscosity

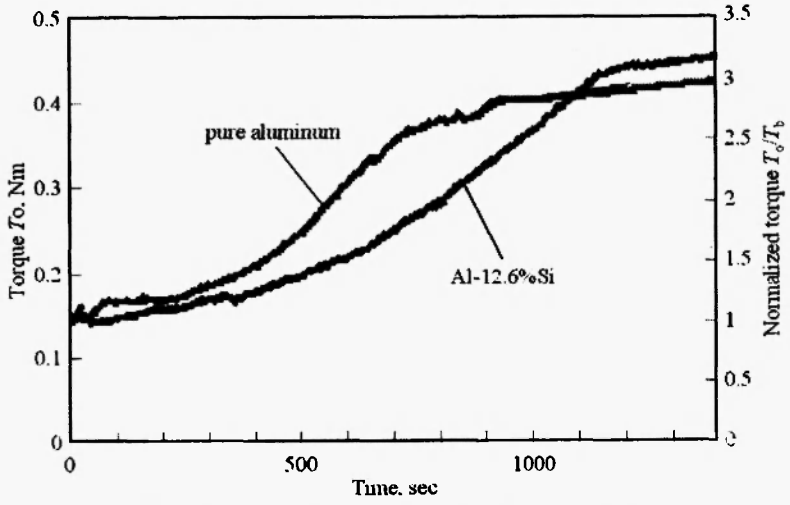


**Fig. 9:** Change in torque of molten alloys with time.

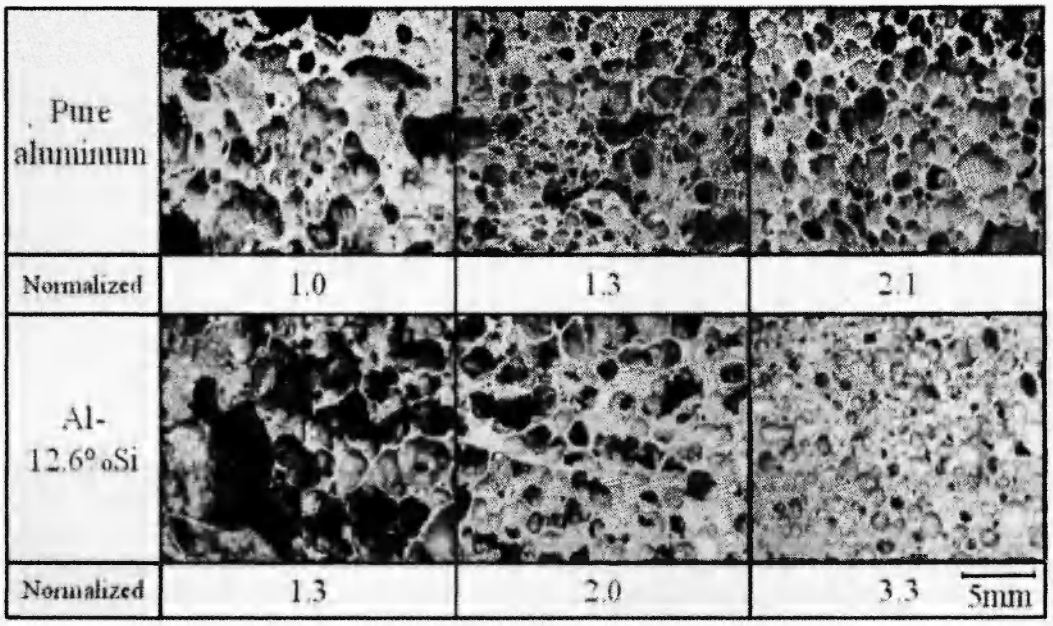


**Fig. 10:** Photos of aluminum foams.

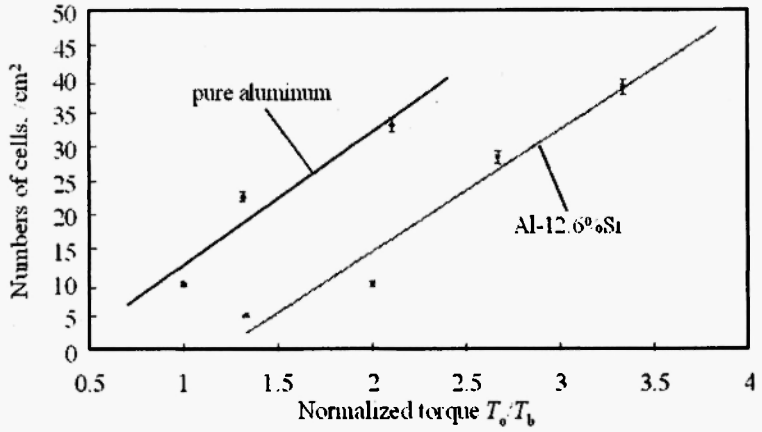


**Fig. 11:** Influence of normalized torque on number of cells per unit area.

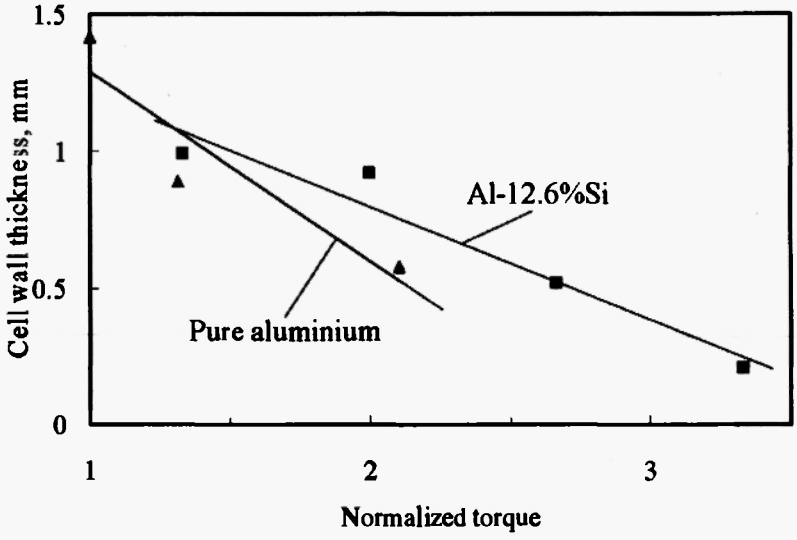


**Fig. 12:** Influence of normalized torque on cell wall thickness

is desirable in order to produce a finer cell size and thinner foam film.

## 6. CONCLUSIONS

The influence of the viscosity on the foamability of aluminum melts was studied using the aqueous solution model on the particle transfer and the powder addition process. Our model shows that the required force for the particle transfer can be calculated based on the contact angle and the size. Based on these results, we proposed a process which effectively entraps non-wetting particles, such as $TiH_2$, aluminum powder and Ca, and uniformly disperses then in the melt.

The influence of the viscosity on the foamability in the aluminum alloys, such as cell size of the foam, was discussed using the optimized stirring process. The results show that the viscosity of the melt is one of the main controlling factors that determine the cell size and the cell wall thickness regardless of the alloy.

## REFERENCES

1. M. F. Ashby *et al.*: *Metal Foams, A Design Model*, Butterworth Heinemann, (2000).
2. D. Exerowa and P. M. Kruglyakov: *Foam and Foam Films Theory, Experiment, Application* Elsevier, (1998).

3. J. Banhart, J. Baumeister and M. Weber: *29th Int'l. Symp. on Automotive Tech. & Automation*, **1,** 611-618 (1996).
4. S. Akiyama *et al.*: US Patent 4 713 277, 1987)
5. E. W. Andrews *et al.*: *Int. J. Mech. Sci.*, **A270**, 113-124 (1999b).
6. P. R. Onck *et al.*: *Int. J. Mech. Sci.*, **43,** 681-699 (2001).
7. H.Nakae *et al.*: *Proc. of ICCM*, **9,** 255-262 (1993).
8. H. Nakae *et al.*: *J. JFS*, **75,** 545-551 (2003).
9. S. W. Ip, Y. Wang and J. M. Toguri: *Canadian Metallurgical Quarterly*, **38,** 81-92 (1999).
10. P. K. Rohatgi *et al.*: *Metallurgical Trans.*, **21A,** 2073-2082 (1990).
11. G. Kaptay: *Metal Matrix Composites for High Performance Applications*, TMS, (2001) pp.71-99.
12. G. Kaptay: *Colloids and Surface*, **A 230,** .67-80 (2003).
13. C. C. Yang and H. Nakae: *J. JFS*, **72,** 593-598 (2000).
14. C. C. Yang and S. C. Chuch: *J. JFS*, **72,** 567-571 (1996).